International Biodeterioration & Biodegradation 158 (2021) 105162

Contents lists available at ScienceDirect

International Biodeterioration & Biodegradation

journal homepage: www.elsevier.com/locate/ibiod

Oxidation states of iron and manganese in lignocellulose altered by the brown rot fungus *Gloeophyllum trabeum* measured *in-situ* using X-ray absorption near edge spectroscopy (XANES)

Samuel L. Zelinka [a,*], Joseph E. Jakes [a], Grant T. Kirker [a], Amy B. Bishell [a], Charles R. Boardman [a], Barry Lai [b], George E. Sterbinsky [b], Jody Jellison [c], Barry Goodell [c]

[a] USDA Forest Service, Forest Products Laboratory, Madison, WI, USA
[b] Advanced Photon Source, Argonne National Laboratory, Lemont, IL, USA
[c] University of Massachusetts, Amherst, MA, USA

ARTICLE INFO

Keywords:
Brown-rot decay
XANES
X-ray fluorescence microscopy
Iron
Manganese
Chelator-mediated fenton

ABSTRACT

Brown rot fungi utilize iron as part of a chelator-mediated Fenton (CMF) reaction during wood biodegradation. Research suggests these fungi reduce Fe^{3+} to promote oxygen radical generation resulting in depolymerization of the wood cell wall. High levels of Mn are also found in wood decayed by brown rot fungi. However, little is known about the oxidation states of Fe and Mn during the decay process. X-ray absorption near edge spectroscopy (XANES) can be used to examine metal oxidation states and coordination chemistry. XANES experiments were conducted on wood decayed by *Gloeophyllum trabeum* over 2–8 weeks with results showing that Mn^{2+} and Fe^{3+} predominated for metal oxidation states. However, Fe^{2+} was present at sites of greater fungal growth In certain cases, the μXANES measurements showed that the fraction of Fe^{2+} in the wood samples was as high as 50%. Localized areas of reduced iron corresponded with areas of greater fungal hyphal mass which is in agreement with how brown rot fungi decay wood via the CMF reaction. The limited change in oxidation state of Mn observed in wood with active fungal activity suggests that the role of manganese in CMF biodegradation chemistry should be further explored.

1. Introduction

Brown rot fungi cause a type of wood decay that results in rapid strength loss of wood in the built environment. Research has shown that brown rot fungi are responsible for 85% of the damage to wood structures caused by decay fungi (Viitanen and Ritschkoff, 1991). Furthermore, brown rot decay can cause large reductions in the strength of lignocellulosic polymers even with low amounts of mass loss (Eaton and Hale, 1993; Green and Highley, 1997; Ibach, 2005).

Understanding the mechanisms involved in the brown rot decay of lignocellulosic polymers remains an active area of research, particularly regarding non-enzymatic catalytic activity. It is generally accepted that the first stage of brown rot decay involves chelator-mediated Fenton (CMF) catalytic degradation where metal ions are used to generate hydroxyl radicals that depolymerize wood (Arantes et al., 2012; Baldrian and Valášková, 2008; Goodell et al., 1997, 2017). Although brown rot fungi translocate many metal cations, such as K and Ca, Fe has a special role as the primary metal known to be involved in CMF degradation (Jellison et al., 1997). Recent reviews of literature on phenolate derivative chelators produced by the brown rot fungi *Gloeophyllum trabeum* (Gt-chelator) have shown that Gt-chelator primarily consists of hydroquinone metabolites such as hydroquinone (HQ) and methoxy catechol (MeC) derivatives (Arantes and Goodell, 2014; Goodell et al., 1997; Jensen Jr. et al., 2001; Paszczynski et al., 1999; Suzuki et al., 2006). The CMF mechanism proposes that fungal HQ/MeC metabolites can reduce Fe^{3+} extracellularly under pH conditions promoted by the fungus, and the reduced iron can then react with H_2O_2 produced by the fungus to start a radical depolymerization of the wood cell wall. Mn is typically associated with white-rot fungal enzymatic action where secreted Mn peroxidase oxidizes Mn^{2+} to a Mn^{3+}/Mn^{4+} state as part of the depolymerization of lignin (Glenn et al., 1986; Hofrichter, 2002). However, Mn oxidation is not strictly associated with white rot fungi as even ascomycete fungi oxidize Mn^{2+} (Saratovsky et al., 2009). Furthermore, Jellison et al. (1992) noted Mn may also play a role in brown rot decay as

* Corresponding author.
E-mail address: samuel.l.zelinka@usda.gov (S.L. Zelinka).

https://doi.org/10.1016/j.ibiod.2020.105162
Received 20 April 2020; Received in revised form 24 November 2020; Accepted 11 December 2020
Available online 23 December 2020
0964-8305/Published by Elsevier Ltd.

Mn levels are greatly elevated in wood decayed by brown rot fungi, although its role is unclear.

A better understanding of these proposed mechanisms can be achieved through visualization of the spatial positioning and oxidation states of metals in wood and fungi during wood decay. Not only could this understanding lead to potential mechanisms for wood protection, but they could also be useful in developing biomimetic methods for lignocellulose biomass conversion (Arantes et al., 2012; Jakes et al., 2016; Ray et al., 2010). Synchrotron based X-ray Fluorescence Microscopy (XFM) and X-ray Absorption Near Edge Spectroscopy (XANES) are uniquely suited for better understanding the role of metals in the decay process. XFM can be used to create sub-micron maps of elemental composition down to trace concentrations. Using XANES, X-ray absorption is examined above and below the K-edge (binding energy of a K-shell electron) and the absorption pattern can be used to determine the oxidation state and coordination chemistry of metals in diverse substrates (Bertsch and Hunter, 2001).

Recently, XFM was used to map the ion concentration profiles produced by the brown-rot decay fungus *Serpula lacrymans* (Wulfen) P. Karst. (1884) at mm and μm length scales (Kirker et al., 2017). Sections cut from decayed wood had elevated levels of Fe in the wood cell wall, and maps of wood with fungal hyphae showed elevated levels of Fe, Mn, Zn, K, Ca. The XFM measurements of Kirker et al. (2017) gave insight into how the fungus was accumulating and distributing metal ions during the decay process. However, since XFM could not detect the oxidation states of the ions, it was not possible to confirm the Fe oxidation state changes associated with the CMF degradation pathways.

Several papers have suggested the use of XANES for understanding the role of Fe, Mn, and S in the wood decay process (Illman and Dowd, 1997; Illman and Bajt, 1997; Schmalenberger et al., 2011). Notably, several review papers by Illman report that XANES measurements of Fe and Mn in decayed wood were conducted as early as the 1990s (Illman and Dowd, 1997; Illman and Bajt, 1997). However, no data are presented in these review papers other than a statement that Fe^{2+}/Fe^{3+} ratio in brown-rot decayed wood is higher than control. Furthermore, the papers cited in the review articles do not contain XANES data but are rather short abstracts of the experimental techniques utilized (Illman et al., 1994, 1995). Given the lack of published data, it is unclear whether Fe or Mn oxidation states change during the decay process and whether these changes can be used to better understand the decay mechanisms.

While there has only been limited work using XANES to understand Fe and Mn cycling in wood decay fungi, XANES has been used extensively for understanding how certain fungi cycle Mn in the soil. XANES was found to be an ideal technique for studying how some types of fungi utilize Mn because the oxidation state can be measured *in situ* without changing the soil moisture content (Thompson et al., 2005). The amount of the most bioavailable form of manganese, Mn^{2+}, can be quite variable in soils. However, most manganese in minerals will be found associated with iron, and in insoluble oxidized states such as Mn^{4+}. Oxidation of soluble Mn^{2+} to Mn^{3+} or Mn^{4+} states in soils is known to be caused by fungi and bacteria (Diaz et al., 2013; Guest et al., 2002). XANES has been used to demonstrate that the take-all disease in wheat caused by *Gaeumanomyces graminis var. tritici* involves the oxidation of bioavailable Mn^{2+} to insoluble Mn^{4+} near the roots of the wheat plant (Schulze et al., 1995a, 1995b; Thompson et al., 2005). These papers illustrate the utility of XANES for exploring how fungi and other microorganisms alter metal oxidation states and highlight its potential utility for better understanding mechanisms of wood decay fungi.

In this work, we used XANES to study the oxidation states of Fe and Mn during wood decay by the brown rot fungus *Gloeophyllum trabeum*. Specimens were grown such that living fungi could be placed in the synchrotron beamline for analysis. Two different beamlines were used so that the XANES patterns could be collected at different length scales; a beam focused to approximately 1 mm was used to measure the overall oxidation state of the Fe and Mn in the bulk decayed wood, while a sub-micron focused beam was also used so that individual features such as hyphae could be examined. For the large field of view technique, measurements were also taken on dried samples to examine whether the oxidation states were different when the fungi were not active. The goal of this work is to better understand the role of transition metals in brown rot decay, with our objective to examine if XANES could detect changes in key transition metal states that are associated with both extracellular enzymatic and non-enzymatic CMF mechanisms proposed to be active during brown rot. Understanding how transition metals undergo oxidation and reduction in fungal environments will help us understand their roles in promoting extracellular enzyme-, and non-enzymatic- activity. Further this understanding will provide tools for harnessing biodegradation mechanisms for both biorefinery and wood protection processes.

2. Materials and methods

2.1. Overview of the measurement techniques

Two related techniques were used to measure the spatial distribution, concentration, and oxidation states of metals within decayed wood; synchrotron based XANES and X-ray Fluorescence Microscopy (XFM). In XFM, a sample is placed in the beam and exposed to a focused X-ray beam. A fluorescence detector is used to collect photons emitted from the sample. The energy of these emitted photons can be deconvoluted to give the elemental composition of that location down to trace concentrations. The sample can then be raster scanned to develop a map of the composition of the sample. Our XANES measurements used a similar (in some cases the same) fluorescence detector and a similar X-ray energy. However, instead of scanning different positions, the X-ray energy was changed at a single position. By measuring fluorescence near the K-edge, information about the metal oxidation state can be obtained.

2.2. Fungal growth conditions

All experiments examined *Gloeophyllum trabeum* (Pers.) Murrill MAD 617. Two different length scales were examined as described below.

The macroscale measurements utilized an X-ray beam approximately 1-mm in diameter and the beam was focused on southern pine (Pinus spp.) cubes of 9 mm per side. The experimental setup in general followed the AWPA E10 soil block assay method (Anon, 2012). However, instead of using flint-glass bottles for the growth chambers, the specimens were grown in a polypropylene cup. Polypropylene cups were filled with soil and distilled water so that conditions proportionally match the E10 standard and were autoclaved prior to inoculation. At inoculation, two 5 mm plugs of fungal mycelium harvested from cultures actively growing on malt agar extract plates were transferred aseptically onto a pre-sterilized 40 × 30 × 3 mm feeder strip (also southern pine) that directly abuts the sample to be exposed. Prepared cups were then placed into an environmental chamber at 27 °C and 70% relative humidity. Fungal inoculations were staggered in order to achieve the exposure times (2, 4, 6, and 8 weeks). Immediately prior to placing the specimen in the beam, a window was cut in the polypropylene cup and replaced with a polyimide film window to allow the beam to fully penetrate the container and impinge on the sample (Fig. 1a). Between 2 and 6 wood block specimens per time point were examined at 2,4,6, and 8 weeks (2, 4,6 and 8w) of growth to allow biological variability to be captured.

The microscopic measurements, hereafter referred to as μXANES were collected from fungi grown on 2 μm thick longitudinal and transverse sections of southern pine. The 2 μm thick sections were cut from small wood cubes in a Leica EM UC7 ultramicrotome (Wetzlar, Germany) fitted with a diamond knife. The 2 μm thick sections were then mounted between aluminum sample holder plates that could easily be attached to the kinematic mount on the beamline. A sacrificial southern pine sample known as a “feeder strip” was mounted to the sample holder immediately adjacent, and in contact with, the 2 μm thick sections. This

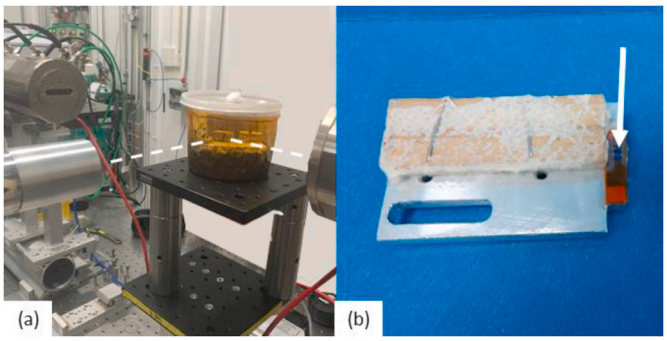

Fig. 1. Experimental setup for the (a) XANES and (b) μXANES measurements. The dotted white line shows the approximate path of the beam from the shutter, to sample impingement, and then to the fluorescence detector. The metal holder for the μXANES measurements was buried in soil to the height of the "feeder strip" so that the fungus could colonize this sacrificial wood strip and then grow into the 2 μm thick wood sections that were placed immediately adjacent to the feeder strip. The white arrow (1b) is pointing to one of the 2 μm thick wood sections.

entire assembly was placed in a sterile growth chamber, with a fungal monoculture of *G. trabeum* (Fig. 1b) used to inoculate the feeder strip. Prior to μXANES analysis, the metal assembly in Fig. 1b was removed from the soil after a set fungal-exposure period of either 2 or 5 weeks, and placed into a humidified chamber within the beam such that the fungal hyphae near the 2 μm thick section were not disturbed. Each time point, 0, 2 and 5 weeks, was represented by 2–3 biological samples. The time points were shorter for these measurements as the 2 μm sections get completely engulfed in hyphae by 8 weeks and the goal was to collect XANES patterns on both the wood and the fungus. A HumidiSys™ relative humidity generator (InstruQuest Inc., Coconut Creek, Florida, USA) supplied with ultra-high purity helium was used to maintain near-saturation humidity conditions allowing the fungus to be imaged in a fully hydrated, and potentially living state. The lack of oxygen in the environment, necessary to prevent beam scattering, likely impacted fungal respiration and growth, but only during the approximate 12–36 h period required for beam exposure.

2.3. XANES measurements

The XANES measurements were performed at beamline 9-BM-C of the Advanced Photon Source located at Argonne National Laboratory. The XANES patterns were collected using a fluorescence detector. For each measurement, multiple (4–6) scans were taken at a single point and then merged into a single curve to reduce noise using the Athena software package (Demeter version 0.9.26) for XAFS processing (Ravel and Newville, 2005). XANES patterns for 2–6 samples each were collected at 2,4,6, and 8 weeks of growth around both the Mn *K*-edge and Fe *K*-edge.

For the Fe XANES, the energy was scanned from 150 eV below the E_o of 7110.75 eV–459.14 eV above the E_o over 511 points. The step size depended on the distance from E_o and was in 5 eV steps from −150eV to −20eV, 0.3eV steps from −20eV to 100eV, and 4.2eV from 100eV to 459.14eV, with a 1s dwell time at each point. The Mn XANES utilized the same step sizes, number of points, and dwell time, but was centered around an E_o of 6537.67 eV.

In addition to testing wood with living fungi, an additional 2–6 wood blocks samples were removed from the growth chambers and the XANES patterns were collected on this material in the dry state. The material was dried by removing the samples from the growth chambers and allowing the samples to air dry. In some cases, the surface hyphae were scraped from the wood samples, and the dried wood with only internal fungal decay hyphae were then analyzed. However, no differences were found between the dried wood samples that were scraped and the samples with surface hyphae, so the raw data for all dry samples were merged into a single XANES pattern for easy comparison. To check for sample damage caused by the beam, living samples were scanned multiple times over a several hour period and no differences could be detected in the XANES pattern suggesting that the beam was not affecting the XANES patterns or the metal oxidation states. Multiple replicates were examined in both the living and dry state with 12–36 individual scans merged to produce final plots. Raw data were normalized using the Athena software package (Ravel and Newville, 2005). The fluorescence signal was divided by incident X-ray beam intensity to produce the X-ray absorption coefficient "$\mu(E)$" as a function of energy. The $\mu(E)$ was then normalized from the pre and post-edge regions to have an edge step of one in Athena.

2.4. μXANES and XFM measurements

The *μXANES* measurements were taken at beamline 2-ID-D of the Advanced Photon Source located at Argonne National Laboratory. The beamline was configured such that maps of the elemental concentrations of several elements important in fungal decay (Ca, Fe, Mn) could also be collected by raster-scanning the sample with the beam energy set to higher than the Fe *K*-edge using XFM.

The experimental procedure involved collecting elemental maps for elements whose K_α peaks were lower than that of Fe using XFM and then targeting specific regions of fungal hyphae or wood cells to collect a XANES pattern. The XFM maps were taken with a dwell time of 5 ms. Several different vertical and horizontal step sizes were used; most maps were collected with step sizes between 0.3 μm and 0.5 μm. The XFM data were analyzed using the MAPS software package where the full fluorescence spectra were fit to modified Gaussian peaks and the background was iteratively calculated and subtracted (Vogt, 2003). The elemental quantification was calibrated by a standard reference (RF4-100-S1749, AXO DRESDEN GmbH, Heidenau, Germany).

Because the beam energy could not be adjusted without re-aligning the beam, only Fe μXANES patterns were collected. The data were collected in 1 eV steps from 7074eV to 7154 eV. The fluorescence signal and upstream ion current were exported from the MAPS software package and normalized in Athena as described earlier.

2.5. Determination of Mn oxidation states

The Mn oxidation states were determined by the method of Schulze et al. (1995b) with the following modifications. Schulze et al. (1995b) calculated the percentage of Mn^{2+} in unknown mixtures by noting that the white line peak of a Mn mixture was linearly related to the fraction of Mn^{2+}. In our work, we established the Mn^{2+} peak at 6551.09 eV as measured from a standard of $MnSO_4{\cdot}H_2O$ (Mn^{2+}) and the Mn^{4+} peak 6560.23 eV was established from a standard of Birnessite ($Na_4Mn_{14}O_{27}{\cdot}9H_2O$). The white line peak ($P_{wl}$, in eV) was then measured for each experimental scan and the fraction of Mn^{2+} was determined from

$$f(Mn^{2+}) = \frac{(P_{wl} - 6560.23)}{6551.09 - 6560.23} \quad \text{Eq (1)}$$

2.6. Determination of Fe oxidation states

The iron oxidation states were determined from the position of the pre-edge centroid, similar to previous work identifying iron oxidation states in soils, aerosols, and tissues (Bajt et al., 1994; Kwiatek et al., 2001; Oakes et al., 2012; Prietzel et al., 2007). The pre-edge feature arises from 1s→3d transitions and the position of the pre-edge centroid depends primarily upon the oxidation state but is also dependent on whether the iron is complexed to organic or inorganic compounds (Prietzel et al., 2007).

The peak of the pre-edge centroid for the XANES spectra was determined in a three-stage process using custom routines constructed using MATLAB (MathWorks, Natick, MA) curve fitting software. Full

details of the program used to locate the centroid position, illustrations of the white line and pre-edge peak positions, and the MATLAB code are provided in the Supplementary Information.

Fe^{2+} oxalate and Fe^{3+} oxalate were used to develop a two point calibration curve for the oxidation states. According to Prietzel et al. (2007), iron oxalates are the ideal model compounds for organic iron oxidation state determination as most organic iron is bound with carboxylic acid groups. The measured centroid position of Fe^{2+} oxalate was 7111.40 eV and the position of Fe^{3+} oxalate was 7113.10 eV. The oxidation state in the sample was then calculated from the following equation:

$$f(Fe^{2+}) = \frac{(C - 7113.10)}{7111.40 - 7113.10} \quad \text{Eq (2)}$$

where C is the pre-edge centroid position in eV and $f(Fe^{2+})$ is the fraction of Fe^{2+} in the sample.

The iron foil white line was calibrated to different energies at 2-ID-D and 9-BM (Kraft et al., 1996). To ensure consistency in the iron-oxidation state analyses, the pre-edge centroids of the 2-ID-D data were shifted. The shift was performed by measuring the pre-edge centroid of Fe^{3+} sulfate and then shifting the measured centroids measured at 2-ID-D so that the Fe^{3+} sulfate occurred at the same energy (7113.32 eV).

3. Results

3.1. Mn XANES

Fig. 2 summarizes the Mn oxidation states measured at 0,2,4,6, and 8w on the bulk wood samples exposed to the fungus. For each condition, the oxidation state was measured for wood samples in the growth chamber with living fungi "wood with active growth", in samples removed from the growth chamber and allowed to dry "dried wood", and in the soil from the growth chamber "soil". Example XANES patterns are presented for the 8 weeks of exposure time point in Fig. 3 for reference along with the standards used to get the oxidation state calibration curves for Birnessite ($Na_4Mn_{14}O_{27}{\cdot}9H_2O$), the Mn^{4+} standard and $MnSO_4{\cdot}H_2O$ (Mn^{2+}) and the white line positions of Mn^{2+} and Mn^{4+} used in Eq. (1).

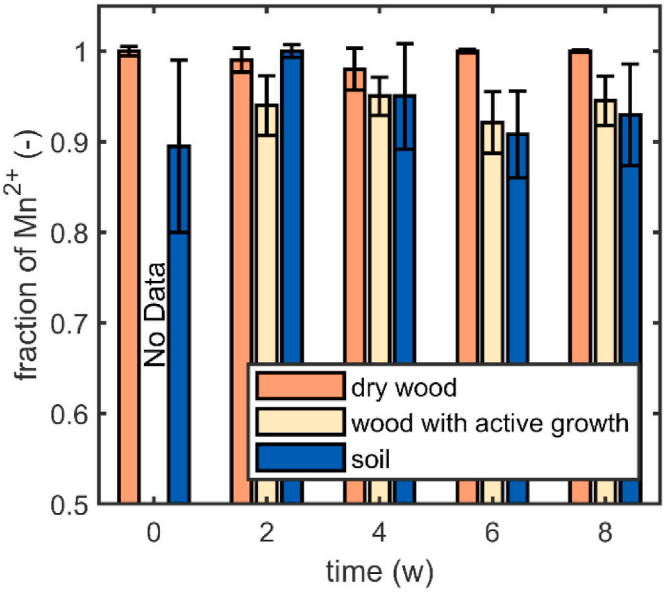

Fig. 2. Summary of the Mn oxidization states measured on macroscopic samples presented as the fraction of Mn^{2+} as determined from the white line peak (Eq (1)) as a function of exposure time and sample condition. "Dry wood" specimens were removed from the growth chamber and tested in a dry state. The "wood with active growth" samples were tested on live fungi within the growth chamber. "Soil" samples were measurements from soil within the growth chambers. Since the "0 w" data are uninoculated controls, there is no data for living fungi at that time period. Error bars represent the standard deviation.

From Fig. 2, it is clear that Mn appears to be in a predominately Mn^{2+} oxidation state for all of the samples. The control wood (labeled "0w" in Fig. 2) contained 100% Mn^{2+}. Similarly, for the blocks that were exposed to *G. trabeum* and then dried (labeled "dried wood" in Fig. 2), the fraction of Mn^{2+} was also very high and approached unity. Both the white line peak and post-edge region appeared like that of the control wood.

For the samples measured in the live/hydrated state (labeled "wood

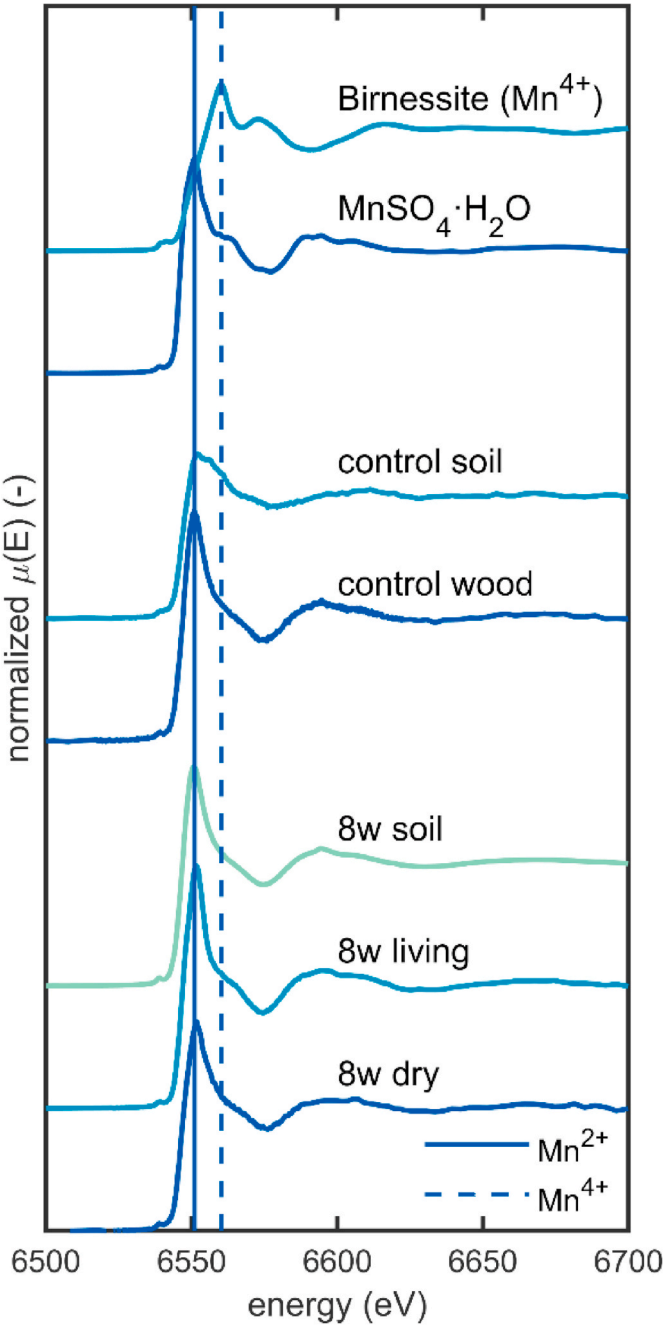

Fig. 3. Example Mn XANES patterns after 8 weeks exposure to *G. trabeum*, along with the control wood, soil, and the Mn^{2+} and Mn^{4+} standards used to calibrate the oxidation state calculation.

with active growth" in Fig. 2), a small fraction of Mn^{4+} was observed. The fraction of Mn^{4+} varied between 5% in the sample exposed for 4 weeks to as high as 8% in the sample exposed for 6 weeks. While the small amount of Mn^{4+} was observable by a slight shift in the white line peak, the post edge region retained most of the features of the $MnSO_4{\cdot}H_2O$ standard. The domination of the spectra by the high fraction of the Mn^{2+} features makes it difficult to make observations on the coordination of the Mn^{4+} in the decaying wood.

3.2. Fe XANES

Fe oxidation states were measured on wood with living decay fungi, wood that had been dried after decay, and soil with living decay fungi at 2,4,6 and 8 weeks. However, unlike the Mn data, which showed a variation in the oxidation state, nearly all the Fe was in the Fe^{3+} oxidation state. The sole exception was the wood blocks exposed to fungus for 8 weeks and then dried, which contained 6% Fe^{2+}.

Example XANES patterns taken from the data at 8w, along with the control data and the iron oxalate standards (Fig. 4) show all spectra appear very similar to the Fe^{3+} oxalate standard. Notably, the white line peak of the 8w dried sample was shifted to a lower energy indicating the presence of more Fe^{2+}. However, the data suggest that nearly all the iron in the other samples assayed was in the Fe^{3+} oxidation state. The control wood, which was not exposed to the fungus, did not have enough iron transported into it to measure a XANES pattern. Iron concentrations in the control sample were measured using XFM. Fe maps of two-micron-thick wood sections were found to contain 0.4–0.6 μmol Fe per g of dried wood. This supports our prior research which demonstrated that a significant amount of iron is translocated by decay fungi, even at exposure periods of only 2w (Kirker et al., 2017). A potential concern in this work is that intense light is known to reduce iron in the presence of oxalate. The fact that we were able to obtain consistent and repeatable Fe^{2+} oxalate XANES patterns in replicates over time, and the fact that the Fe^{2+} oxalate data collected closely matches previously published Fe^{2+} oxalate XANES patterns, demonstrates that the beam was not photo-oxidizing the iron oxalate in the sample to a Fe^{3+} oxidation state. We conclude therefore that the majority of the iron in wood inoculated with *G trabeum* on the macroscopic level has an Fe^{3+} oxidation state with patterns similar to the Fe^{3+} oxalate standard.

3.3. Fe μXANES

Fe μXANES measurements were performed on hydrated fungi grown on 2 μm thick sections of wood. Because these scans had a low signal-to-noise ratio at this level of resolution, many μXANES spectra were too noisy to analyze and the pre-edge centroid could not be determined. Of the 146 scans collected, only 25 scans had a sufficient signal to noise ratio to locate a pre-edge centroid with the MATLAB code presented in the *Supplementary Information* without having the code select peaks outside the limits of the curve fitting bounds. The 25 scans represented 3 different biological samples at both 2w and 5w. Attempts were made to measure the XANES pattern of "control" wood without decay; however, as with the large-scale measurements, there was not enough Fe in these samples to collect a XANES pattern. Measurable amounts of Fe^{2+} were detected in the samples at 5w exposure; at 2w exposure only three scans showed measurable amounts of iron and in all three of these scans the amount of Fe^{2+} was less than 40% (Fig. 5).

A unique aspect of μXANES analysis is that measurements can be taken on specific features within the fungal hyphal mass and the decayed wood located in the XFM maps. We used this technique to examine our hypothesis that different regions or features within wood or hyphal mass may have different metal oxidation states. XFM maps for samples exposed for 5 weeks are shown in Fig. 6 which show XFM maps of Fe, Mn and Ca along with corresponding μXANES measurement positions; the XANES measurements in Fig. 6a show a much higher amount of Fe^{2+} than the measurements in Fig. 6b. The relative sizes of Fig. 6a and b are a result of scan areas selected at the beam and represent the full field of view imaged for XANES scan locations.

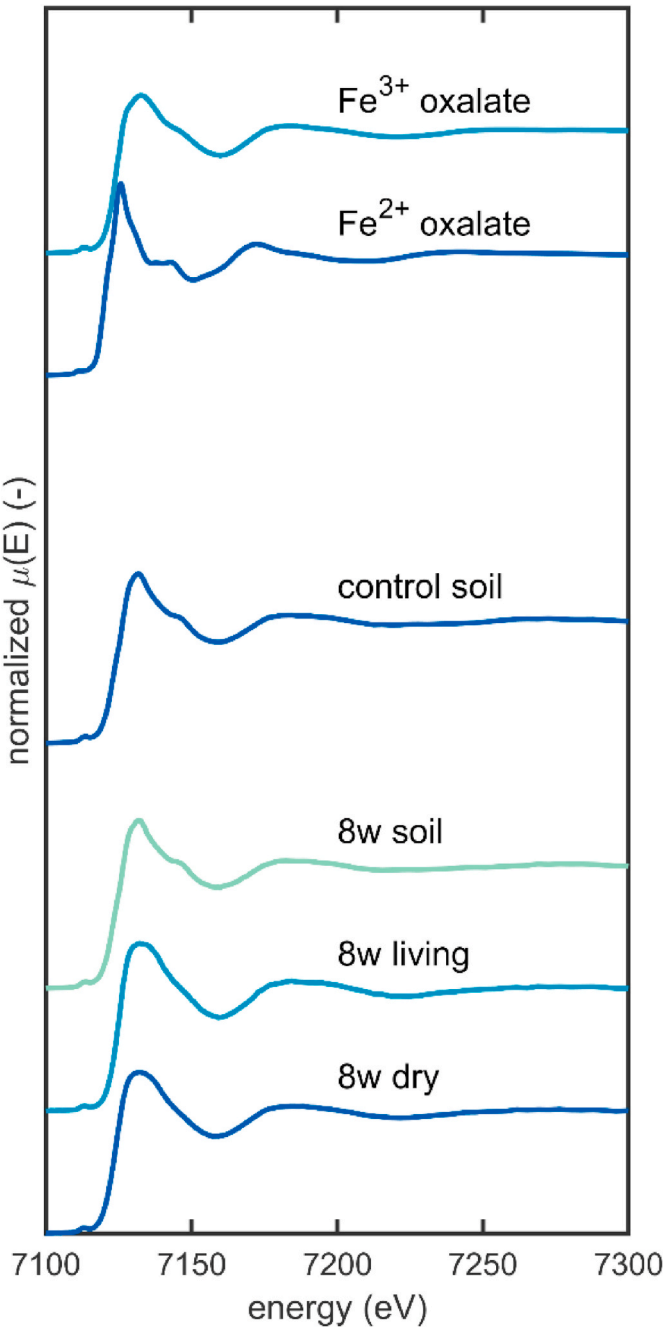

Fig. 4. Fe XANES patterns after 8 weeks exposure to *G. trabeum*, along with data from the control soil and the Fe^{2+} and Fe^{3+} standards used to calibrate the oxidation state calculation. There was not enough iron in the control wood to measure a XANES pattern.

Fig. 6a is a scan of a wide area of fungal growth. No wood cell wall features can be seen in the figure as fungal hyphae overlaying the wood obscure the wood features in most locations. There is a large hyphal mat visible in the left side of the figure as evidenced by the large region of high iron concentration and high amounts of total scattering. On the right side of the image there appears to be less fungal growth and some areas with empty space in between hyphae. In addition, there is another agglomeration (mat) of hyphae on the far right side of the image, oriented in a diagonal strip. Four XANES scans were taken at various features in the large hyphal mat and on the diagonal agglomeration of

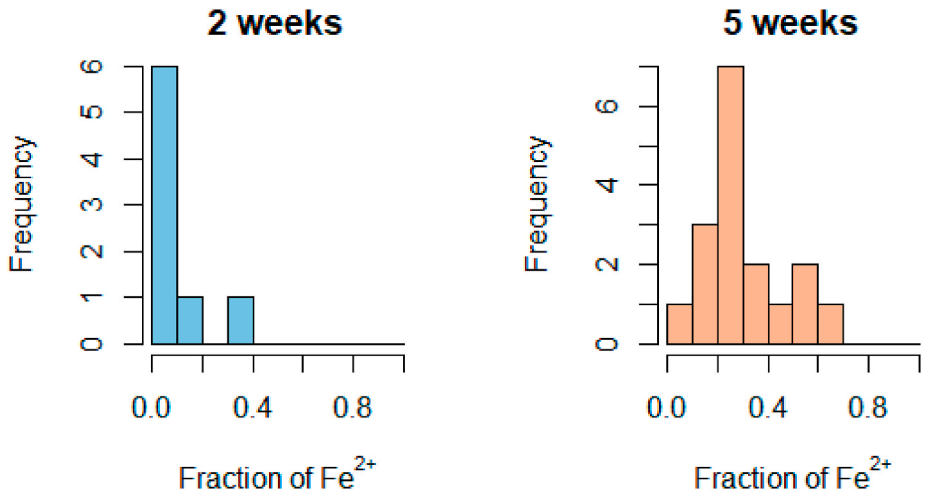

Fig. 5. Histogram showing the distribution of Fe^{2+} from μXANES scans taken at 2 weeks and 5 weeks of exposure.

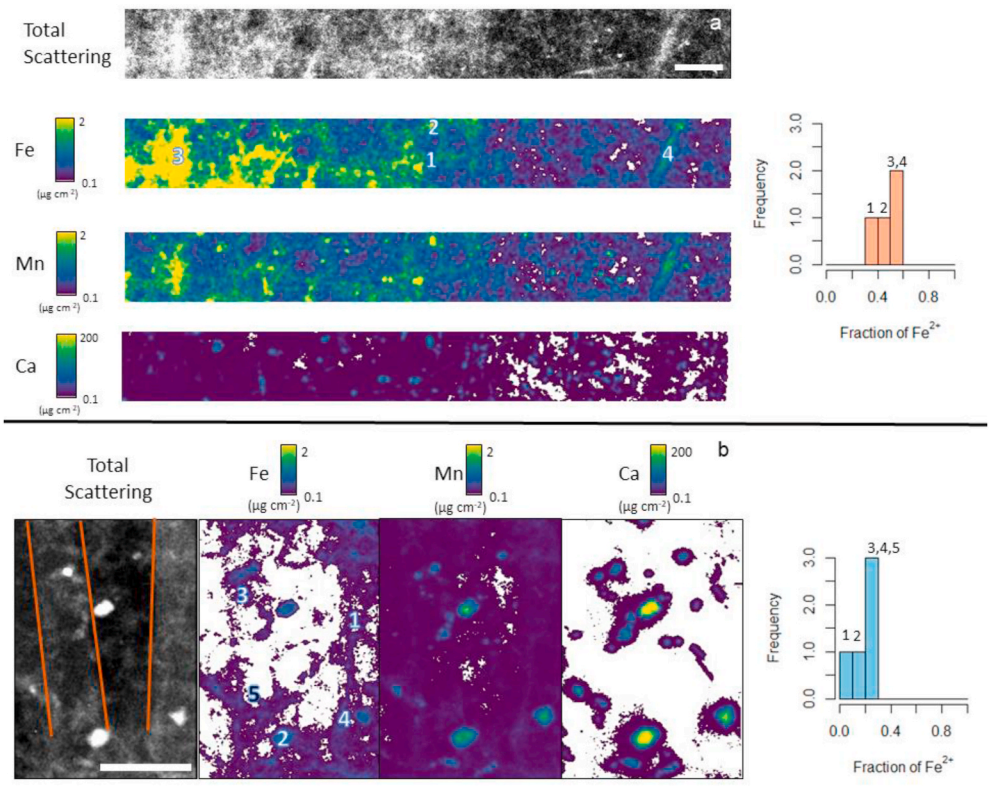

Fig. 6. XFM maps of the total scattering, Fe, Mn, and Ca at 5w exposure. The numbers mark the positions of XANES scans. 4(a) The image contains a large hyphal mat on the left side of the image and another smaller diagonal strip of hyphae mat on the right side. 4 (b) At left, the orange lines outline the wood cell walls. The white numbers mark the positions of XANES scans and are placed over the histograms so that the fraction of Fe^{2+} at each location can be determined. The scale bars are 50 μm long. (For interpretation of the references to colour in this figure legend, the reader is referred to the Web version of this article.)

hyphae; the scan locations are indicated with numbers on Fig. 6a. Locations 3 and 4 had 60% Fe^{2+} and locations 1 and 2 had 30–40% Fe^{2+}.

In contrast to the sample material in Fig. 6a, the material in Fig. 6b had much less fungal growth. In this image, which is at higher spatial resolution than that in Fig. 6a, the wood cell wall is visible as regions of higher total scattering. The region was identified as being part of the cell wall because of its size, straightness, and orientation were similar to how the sample was placed on the sample holder and previous XFM images of wood cell walls. The positions of the wood cell walls are highlighted with orange lines in Fig. 6b and the dark area between these lines in the total scattering image is the cell lumen. The total scattering also contained bright regions, with corresponding high concentrations of Ca, and to a lesser extent, Fe and Mn. Similar features have been observed in XFM maps of decayed wood and were identified as oxalate crystals (Kirker et al., 2017). Brown rot fungi secrete oxalate and other low molecular weight chelators to regulate the CMF reaction and excess oxalate has been observed to form crystals in decayed wood (Goodell et al., 1997; Kirker et al., 2017; Paszczynski et al., 1999). XANES measurements were taken in regions along the cell wall with varying amounts of Fe and on oxalate crystals. In addition to having much less fungal growth than Fig. 6a, the average oxidation states measured in Fig. 6b were lower than those measured in Fig. 6a with the mean measurement containing 20% Fe^{2+} compared to a mean value of 50% Fe^{2+} for the measurements taken on features in Fig. 6a. The measurement at Location 1 had no detectable Fe^{2+}.

4. Discussion

4.1. Mn oxidation states

Mn was found to be predominately in an Mn^{2+} oxidation state for all of the samples. A limited amount of Mn^{4+} (up to 8% of total Mn) was observed in blocks with living fungi. In general, the samples exposed to fungus and then dried had the highest fraction of Mn^{2+} and for all time points observed except 2w, the fraction of Mn^{2+} was similar across the soil and the samples with living fungi. *G. trabeum* is not a white rot fungus and it has no genes encoding Mn peroxidase enzymes. Keiluweit et al. (2015) found that litter decomposing fungi of unknown species were associated with Mn oxidation over longer periods of time when more organic matter was present. It is possible that, with longer exposures with more organic matter that our work may have shown similar trends.

In the decayed wood, a limited amount of Mn^{4+} was observed, possibly due to brown rot fungal action, but it is currently unclear how much of the change noted may be caused by the fungus. The cycling of Mn (from Mn^{2+} to Mn^{4+}) has not previously been reported associated with brown rot biodegradation of wood although manganese redox cycling with certain chelators is known. This suggests that further research with Mn should be conducted in the future to determine if a Mn cycle is associated in some cases with the Fe-CMF cycle, which might enhance or regulate brown rot fungal biodeterioration under some environmental conditions.

4.2. Fe oxidation states

The resolution of the XFM images and *μXANES* measurements do not easily lend themselves to the identification of hyphal features (which are typically less than 4 μm in diameter (Wilcox, 1993)). Furthermore, corresponding light microscopy could not be performed on the same samples, as drying would greatly affect the size and geometry of the fungal growth. While we were not able to correlate the measured oxidation state to individual hyphal features, in general, some trends can be observed in the μXANES spectra. The amount of Fe^{2+} appears to correlate with the amount of fungal growth and the transport of iron into the wood samples by fungal hyphae. Samples measured at 2w of growth had little or no detectable Fe^{2+} (Fig. 5). Furthermore, within the variation of samples measured at 5w, the amount of Fe^{2+} was higher in regions where there was more fungal growth, as noted by the total scattering and Fe concentration (See Fig. 6). Finally, the amount of Fe^{2+} does not appear to vary greatly between the calcium oxalate crystals and the fungal growth next to the crystals. Macroscopically, the XANES measurements showed that nearly all of the Fe was in the Fe^{3+} state except for a small amount detected in the sample exposed for 8w and then dried.

In general, these features are consistent with the macroscopic measurements and our understanding of CMF biodegradation of wood by brown rot fungi. Our understanding of CMF degradation in wood suggests that Fe^{2+} is transient and rapidly cycles back to Fe^{3+} during the decay process (Arantes and Goodell, 2014; Goodell et al., 2017; Liu et al., 2020). In the macroscopic measurements on living fungi, it appears that the majority of the iron sampled was in the ferric state for much of the time the samples were analyzed. These μXANES measurements on living brown rot fungi were able to detect some regions of reduced Fe, and the amount of Fe^{2+} was generally correlated with the amount of fungal growth. This is consistent with how we would expect brown rot fungi to employ low molecular weight metabolites to redox cycle with iron in the non-enzymatic CMF biodegradation mechanism.

5. Conclusions

Fe-μXANES analyses showed measurable amounts of reduced Fe^{2+} which correlated with the amount of fungal growth, which supports the role of Fe cycling in CMF brown rot biodegradation mechanisms. In contrast, Mn^{4+} did not increase with additional fungal exposure time during fungal biodegradation of wood.

Declaration of competing interest

The authors declare that they have no known competing financial interests or personal relationships that could have appeared to influence the work reported in this paper.

Acknowledgements

This research used resources of the Advanced Photon Source, a U.S. Department of Energy (DOE) Office of Science User Facility operated for the DOE Office of Science by Argonne National Laboratory under Contract No. DE-AC02-06CH11357. The authors acknowledge the machine shop at the Forest Products Laboratory for manufacture of the metal μXANES holders. We also acknowledge support from the National Institute of Food and Agriculture, U.S. Department of Agriculture, the UMass Center for Agriculture, Food and the Environment under project number S1075 - MAS00503. The contents are solely the responsibility of the authors and do not necessarily represent the official views of the USDA or NIFA.

Appendix A. Supplementary data

Supplementary data to this article can be found online at https://doi.org/10.1016/j.ibiod.2020.105162.

References

Anon, 2012. AWPA E-10: Standard Method for Testing of Wood Preservatives by Laboratory Soil-Block Cultures. American Wood Protection Association, Selma, AL.
Arantes, V., Goodell, B., 2014. Current Understanding of Brown-Rot Fungal Biodegradation Mechanisms: A Review, Deterioration and Protection of Sustainable Biomaterials. American Chemical Society, pp. 3–21.
Arantes, V., Jellison, J., Goodell, B., 2012. Peculiarities of brown-rot fungi and biochemical Fenton reaction with regard to their potential as a model for bioprocessing biomass. Appl. Microbiol. Biotechnol. 94, 323–338.
Bajt, S., Sutton, S., Delaney, J., 1994. X-ray microprobe analysis of iron oxidation states in silicates and oxides using X-ray absorption near edge structure (XANES). Geochem. Cosmochim. Acta 58, 5209–5214.
Baldrian, P., Valášková, V., 2008. Degradation of cellulose by basidiomycetous fungi. FEMS Microbiol. Rev. 32, 501–521.
Bertsch, P.M., Hunter, D.B., 2001. Applications of synchrotron-based X-ray microprobes. Chem. Rev. 101, 1809–1842.
Diaz, J.M., Hansel, C.M., Voelker, B.M., Mendes, C.M., Andeer, P.F., Zhang, T., 2013. Widespread production of extracellular superoxide by heterotrophic bacteria. Science 340, 1223–1226.
Eaton, R.A., Hale, M.D., 1993. Wood: Decay, Pests and Protection. Chapman and Hall Ltd, London.
Glenn, J.K., Akileswaran, L., Gold, M.H., 1986. Mn (II) Oxidation Is the Principal Function of the Extracellular Mn-Peroxidase from Phanerochaete Chrysosporium. Biophysics vol. 251, 688–696.
Goodell, B., Jellison, J., Liu, J., Daniel, G., Paszczynski, A., Fekete, F., Krishnamurthy, S., Jun, L., Xu, G., 1997. Low molecular weight chelators and phenolic compounds isolated from wood decay fungi and their role in the fungal biodegradation of wood. J. Biotechnol. 53, 133–162.
Goodell, B., Zhu, Y., Kim, S., Kafle, K., Eastwood, D., Daniel, G., Jellison, J., Yoshida, M., Groom, L., Pingali, S.V., O'Neill, H., 2017. Modification of the nanostructure of lignocellulose cell walls via a non-enzymatic lignocellulose deconstruction system in brown rot wood-decay fungi. Biotechnol. Biofuels 10, 179.
Green, F., Highley, T.L., 1997. Mechanism of brown-rot decay: paradigm or paradox. Int. Biodeterior. Biodegrad. 39, 113–124.
Guest, C.A., Schulze, D.G., Thompson, I.A., Huber, D.M., 2002. Correlating manganese X-ray absorption near-edge structure spectra with extractable soil manganese. Soil Sci. Soc. Am. J. 66, 1172–1181.
Hofrichter, M., 2002. Lignin conversion by manganese peroxidase (MnP). Enzym. Microb. Technol. 30, 454–466.
Ibach, R.E., 2005. Chapter 5. Biological properties. In: Rowell, R.M. (Ed.), Handbook of Wood Chemistry and Wood Composites. CRC Press, Boca Raton, p. 99.
Illman, B., Bajt, S., Nuessle, P., 1995. Micro-XANES of Iron Redox States in Wood during Degradation by Fungi. Activity Report #BNL-B-1226, National Synchrotron Light Source Activity Report. Brookhaven National Laboratory, Brookhaven, NY.
Illman, B., Dowd, B., 1997. Synchrotron applications in forestry and forest products. Synchrotron Radiat. News 10, 18–23.

Illman, B., Schulze, D.G., Bajt, S., Sutton, R., 1994. Manganese Dectection in Wood Using X-Ray Absorption Near Edge Structure. Activity Report #BNL-52455, National Synchrotron Light Source Activity Report. Brookhaven National Laboratory, Brookhaven, NY.

Illman, B.L., Bajt, S., 1997. Nondestructive elemental analysis of wood biodeterioration using electron paramagnetic resonance and synchrotron X-ray fluorescence. Int. Biodeterior. Biodegrad. 39, 235–242.

Jakes, J.E., Arzola, X., Bergman, R., Ciesielski, P., Hunt, C.G., Rahbar, N., Tshabalala, M., Wiedenhoeft, A.C., Zelinka, S.L., 2016. Not just lumber—using wood in the sustainable future of materials, chemicals, and fuels. JOM 68, 2395–2404.

Jellison, J., Connolly, J., Goodell, B., Doyle, B., Illman, B., Fekete, F., Ostrofsky, A., 1997. The role of cations in the biodegradation of wood by the brown rot fungi. Int. Biodeterior. Biodegrad. 39, 165–179.

Jellison, J., Smith, K.C., Shortle, W.T., 1992. Cation Analysis of Wood Degraded by White-And Brown-Rot Fungi. Document-The International Research Group on Wood Preservation (Sweden). No. 1552.

Jensen Jr., K.A., Houtman, C.J., Ryan, Z.C., Hammel, K.E., 2001. Pathways for extracellular Fenton chemistry in the brown rot basidiomycete Gloeophyllum trabeum. Appl. Environ. Microbiol. 67, 2705–27011.

Keiluweit, M., Nico, P., Harmon, M.E., Mao, J., Pett-Ridge, J., Kleber, M., 2015. Long-term litter decomposition controlled by manganese redox cycling. Proc. Natl. Acad. Sci. Unit. States Am. 112, E5253–E5260.

Kirker, G., Zelinka, S., Gleber, S.-C., Vine, D., Finney, L., Chen, S., Hong, Y.P., Uyarte, O., Vogt, S., Jellison, J., Goodell, B., Jakes, J.E., 2017. Synchrotron-based X-ray fluorescence microscopy enables multiscale spatial visualization of ions involved in fungal lignocellulose deconstruction. Sci. Rep. 7, 41798.

Kraft, S., Stümpel, J., Becker, P., Kuetgens, U., 1996. High resolution x-ray absorption spectroscopy with absolute energy calibration for the determination of absorption edge energies. Rev. Sci. Instrum. 67, 681–687.

Kwiatek, W., Gałka, M., Hanson, A., Paluszkiewicz, C., Cichocki, T., 2001. XANES as a tool for iron oxidation state determination in tissues. J. Alloys Compd. 328, 276–282.

Liu, J., Zhu, Y., Wang, C., Goodell, B., Esker, A., 2020. Chelator-mediated biomimetic degradation of cellulose and chitin. Int. J. Biol. Macromol. https://doi.org/10.1016/j.ijbiomac.2020.02.262.

Oakes, M., Weber, R., Lai, B., Russell, A., Ingall, E., 2012. Characterization of iron speciation in urban and rural single particles using XANES spectroscopy and micro X-ray fluorescence measurements: investigating the relationship between speciation and fractional iron solubility. Atmos. Chem. Phys. 12, 745–756.

Paszczynski, A., Crawford, R., Funk, D., Goodell, B., 1999. De novo synthesis of 4,5-dimethoxycatechol and 2,5-dimethoxyhydroquinone by the Brown rot fungus *Gloeophyllum trabeum*. Appl. Environ. Microbiol. 65, 674–679.

Prietzel, J., Thieme, J., Eusterhues, K., Eichert, D., 2007. Iron speciation in soils and soil aggregates by synchrotron-based X-ray microspectroscopy (XANES, μ-XANES). Eur. J. Soil Sci. 58, 1027–1041.

Ravel, B., Newville, M., 2005. ATHENA, ARTEMIS, HEPHAESTUS: data analysis for X-ray absorption spectroscopy using IFEFFIT. J. Synchrotron Radiat. 12, 537–541.

Ray, M.J., Leak, D.J., Spanu, P.D., Murphy, R.J., 2010. Brown rot fungal early stage decay mechanism as a biological pretreatment for softwood biomass in biofuel production. Biomass Bioenergy 34, 1257–1262.

Saratovsky, I., Gurr, S.J., Hayward, M.A., 2009. The structure of manganese oxide formed by the fungus Acremonium sp. strain KR21-2. Geochem. Cosmochim. Acta 73, 3291–3300.

Schmalenberger, A., Pritzkow, W., Ojeda, J.J., Noll, M., 2011. Characterization of main sulfur source of wood-degrading basidiomycetes by S K-edge X-ray absorption near edge spectroscopy (XANES). Int. Biodeterior. Biodegrad. 65, 1215–1223.

Schulze, D., McCay-Buis, T., Sutton, S., Huber, D., 1995a. Manganese Oxidation States in Gaeumannomyces-Infested Wheat Rhizospheres Probed by Micro-XANES Spectroscopy. Phytopathology (USA).

Schulze, D., Sutton, S., Bajt, S., 1995b. Determining manganese oxidation state in soils using X-ray absorption near-edge structure (XANES) spectroscopy. Soil Sci. Soc. Am. J. 59, 1540–1548.

Suzuki, M.R., Hunt, C.G., Houtman, C.J., Dalebroux, Z.D., Hammel, K.E., 2006. Fungal hydroquinones contribute to brown rot of wood. Environ. Microbiol. 8, 2214–2223.

Thompson, I.A., Huber, D.M., Guest, C.A., Schulze, D.G., 2005. Fungal manganese oxidation in a reduced soil. Environ. Microbiol. 7, 1480–1487.

Viitanen, H., Ritschkoff, A., 1991. Brown Rot Decay in Wooden Constructions. Effect of Temperature, Humidity and Moisture. Rapport-Sveriges Lantbruksuniversitet, Institutionen foer Virkeslaera. Sweden.

Vogt, S., 2003. MAPS: a set of software tools for analysis and visualization of 3D X-ray fluorescence data sets. J. Phys. IV 104, 635–638.

Wilcox, W.W., 1993. Comparative morphology of early stages of brown-rot wood decay. IAWA J. 14, 127–138.